Hindawi
Scientific Programming
Volume 2022, Article ID 4633128, 8 pages
https://doi.org/10.1155/2022/4633128

Research Article

Finite Element Analysis Model Design on the Mechanical Properties of Prefabricated Shear Wall Structure

Yuan Zhang

Faculty of Architecture and Civil Engineering, Huaiyin Institute of Technology, Huai'an 223001, Jiangsu, China

Correspondence should be addressed to Yuan Zhang; zhyuang111@hyit.edu.cn

Received 31 July 2022; Revised 14 August 2022; Accepted 23 August 2022; Published 10 October 2022

Academic Editor: Lianhui Li

At present, the mechanical properties analysis method of prefabricated shear wall structure based on static test is low overall simulation precision. In this paper, the finite element method is used to analyze the force performance of the prefabricated shear wall structure. Based on the shear of concrete material, elastic modulus, Poisson ratio, open fracture, the transfer coefficients of open and closed fracture, and tensile strength parameters, the finite element model is established by ANSYS. The vertical load and the horizontal load of the prefabricated shear wall structure are calculated, and the limit load value is obtained. The maximum stress change of the connector, the energy dissipation of the shear wall structure, and the change of the equivalent viscous damping coefficient are obtained by the way of loading and displacement change. The experimental results show that the simulated values of stiffness degradation, maximum displacement, maximum strain, and stress distribution obtained by this method are in good agreement with the actual values and are reliable.

1. Introduction

Along with city development scale in China more and more big, the requirements of the government for environmental protection are higher, the requirements of real estate developers for time, cost, and quality are more strict, and the requirements of owners for the building product safety and comfort performance gradually increase, which have become the bottleneck restricting the development of the construction industry [1, 2]. The prefabricated shear wall structure has come into being. The fabricated building is a building constructed by precast components at the site. It has the advantages of short construction period, high construction quality, and environmental protection. It is catering to the national policies and development requirements of housing industrialization and building energy conservation and emission reduction. With the continuous development of prefabricated shear wall structure, the stress analysis has become a hot issue in structural engineering [3, 4].

Zhang et al. [5] put forward an assembly scheme for the external wall panel for steel structure. In order to study the lateral resistance and seismic performance of steel frames with such wall panels, the ABAQUS finite element software was used to establish the overall model and comparison model of steel frames, and the finite element analysis of uniaxial loading and low cycle reciprocating loading was carried out. The results showed that the connection of the outer wall panel could guarantee the connection between the outer wall plate and the steel frame. When the structure had large deformation under lateral load, it could limit the transfer force between the wall panels and the frames, ensured that the wall panels were in an elastic state, and avoided wall panels from falling down. The enclosure system consisting of the external wall panel and the connection node significantly improved the mechanical performance of the steel frame, the initial stiffness of the structure was increased by 1.18 times, and the bearing capacity was increased by more than 30%. The scheme could enhance the seismic performance of the structure. When simulating the low cycle reciprocating loading, the total energy dissipation of the external wall panel's steel frame model was increased by more than 90% compared with the pure frame model, but the overall simulation result was quite different from the actual value.

In view of the large discrepancy between the simulation results in the literature and the actual values, a new finite element analysis method of prefabricated shear wall structure is put forward to improve the accuracy of mechanical properties of shear wall structure analysis.

2. Finite Element Analysis of the Mechanical Properties of Prefabricated Shear Wall Structure

The prefabricated shear wall structure is a new type of wallboard. The width of a single plate with a binding body part is selected as an analysis unit. Its size is the length of 3000 mm, the width of 600 mm, the thickness of 200 mm, and the concrete grade is C30. Because the integral modeling of ANSYS is used, the reinforcement ratio of the vertical bar in the plate is 1%, and the reinforcement ratio of the horizontal bar is 0.25%.

The material parameters in finite element analysis are as follows: concrete C30, elastic modulus 3.0 GPa, Poisson's ratio 0.2, steel bar HRB335, opening crack's shear transfer coefficient 0.35, closed crack's shear transfer coefficient 0.95, and the tensile strength 1.43 MPa.

2.1. The Model is Established

2.1.1. Defining the Element Properties. The concrete is defined, the distribution unit type is SOLID65 unit, and the proper real constant and material model are selected. In considering the reinforced modeling, the internal structure of the structure is defined by the reinforcement ratio of the longitudinal reinforcement and the distribution of reinforcement in the real constant [6].

2.1.2. The Division of Grid. The grid division is divided by swept grid and the source surface grid is divided by the mapped grid. The grid precision is controlled within 100 mm [7].

2.1.3. Applying Constraint and Loads. This model is loaded by force mode. The rigid pad is added to the local compression position. The shell 63 element is adopted to prevent the stress concentration to cause that the calculation does not converge.

A fixed end is applied at the bottom of the wallboard, and the top is the free end.

2.2. Solving and Postprocessing. The nonlinear analysis of the wall panel is carried out, and the mechanical properties of the components in the force process are obtained through the general postprocessing and the time postprocessing.

In addition, the prefabricated shear wall model structure is shown in Figure 1.

The single axis strain-stress relation diagram of the concrete in Figure 1 is shown in Figure 2(a), and the stress-strain curve of steel bar is shown in Figure 2(b).

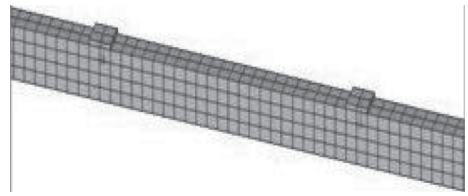

Figure 1: Finite element model of prefabricated shear wall structure.

According to the provisions of the "Technical specification for concrete structure of high rise buildings," under the action of representative value of neutral load, the axial pressure of the one, two, and three grade shear wall limbs is not suitable for the following restrictions: first class (9°): the limit of corresponding axial-compression ratio is 0.4, another level (6°, 7°, and 8°) the limit of corresponding axial-compression ratio is 0.5, and the limit of the axial compression ratio of second or third level is 0.6.

In this paper, the axial compression ratio is 0.4, 0.5, and 0.6 [8], and the vertical load of the prefabricated shear wall structure is calculated according to formula (1).

$$\mu = \frac{N}{(f_c * A)}, \tag{1}$$

where A represents the area of the full section of the shear wall, N represents the axial pressure value of the section of shear wall, and μ represents the load value.

According to the formula (1), there are

$$\begin{aligned} N_1 &= 0.4 * f_c * A = 686\text{kN}, \\ N_2 &= 0.5 * f_c * A = 859\text{kN}, \\ N_3 &= 0.6 * f_c * A = 1030\text{kN}. \end{aligned} \tag{2}$$

Through the above calculation, the maximum bearing capacity of the vertical load of the prefabricated shear wall structure is 1030 kN. According to the provisions of the "Technical specification for concrete structure of high rise buildings," the maximum horizontal displacement and height ratio $\Delta\mu/h$ of the floor layer between the floor layers under the stress load calculated by the elastic method conform to Table 1 [9, 10].

According to Table 1, the calculated maximum displacement of the wall panel is 3 mm. When the vertex displacement of 3 mm can be obtained by using the formula (3), the horizontal load of the prefabricated shear wall structure is 36 kN, that is, the horizontal load under normal serviceability limit state.

$$w_{\max} = \frac{Fl}{EI}, \tag{3}$$

where F represents the load on the model, l represents the length of the model after the deformation, E represents the modulus of elasticity of the model, and I represents the I shaped section of the model.

According to "The technical regulations of high building concrete structure," there are as follows:

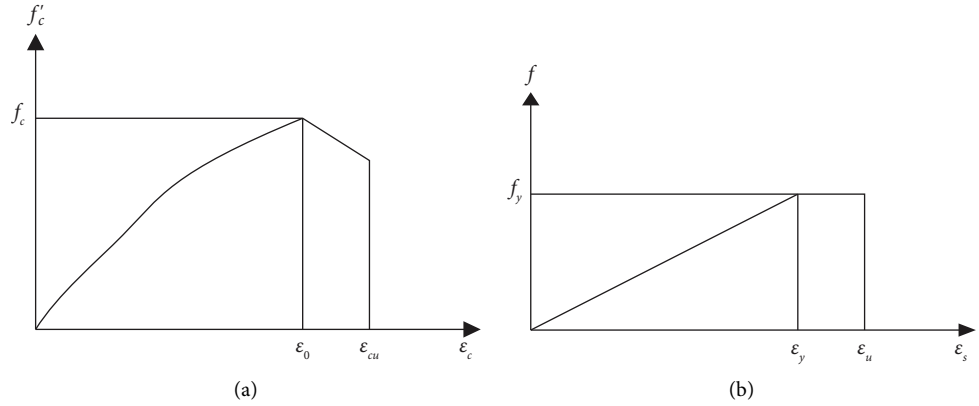

Figure 2: The stress-strain curve of material. (a)Single axis stress-strain relation diagram of concrete and (b) stress-strain curve of steel bar.

Table 1: Ratio of maximum horizontal displacement to height.

Structural system	$\Delta\mu/h$ limit
Frame	1/550
Frame-shear wall, frame-core tube, and flat plate-column-shear wall	1/800
Tube in tube, shear wall	1/1000
The transformation layer other than the frame structure	1/1000

$$V \leq \frac{1}{\lambda - 1}\left(0.5 f_y * b * h + 0.13N\frac{A_w}{s}h\right), \tag{4}$$

where V represents displacement, A_w represents the area of I shaped or T shaped cross-section shear wall, λ represents the shear span ratio of section, s represents the horizontal distribution of reinforcement spacing of shear wall, b represents the section width, and h represents the effective height of the model.

According to formula (4), the shear capacity of the prefabricated shear wall structure is 123.8 kN; that is, the horizontal load under the ultimate bearing capacity of the prefabricated shear wall structure.

Figure 3 is the maximum stress change of the perforated rebar in the prefabricated shear wall structure, and Figure 4 is the maximum stress change of the connecting steel plate.

According to Figures 3 and 4, it is known that at the initial stage of loading displacement, the connections are in the elastic deformation stage. When the displacement is loaded to 25 mm, the maximum stress of the connecting steel plate is 227 Mpa and enters the yield stage. Then, when the displacement is loaded to 45 mm, the perforated rebar enters the yield stage, and the maximum stress is 380 Mpa. When the displacement is loaded to 52 mm, the maximum stress of the steel plate begins to increase and enters the stage of plastic hardening. When the displacement is loaded to 55 mm, the perforated rebar enters the plastic hardening stage. When the displacement is loaded to 75 mm, the connecting steel plate reaches the limit stress 310 Mpa and enters the necking deformation stage. When the specimen is completely destroyed, the connecting steel plate is completely broken, but the reinforcing bar does not destroy.

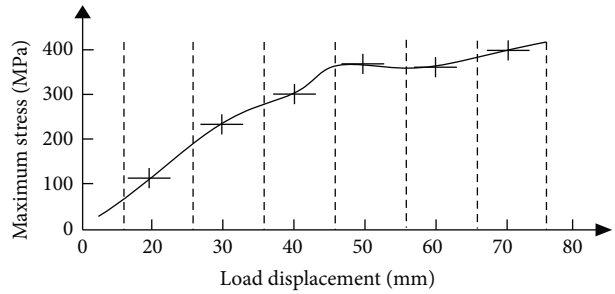

Figure 3: The maximum stress change of perforated rebar.

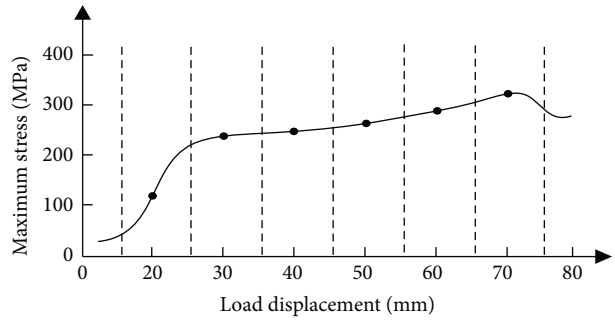

Figure 4: Maximum stress change of connecting steel plate.

There are two main reasons for structural vibration energy dissipation: structural damping energy dissipation and elastoplastic energy dissipation.

Damping and elasticity are one of the most important properties of the structure. When the structure is in the case of elastic vibration, the damping causes the dissipation of the structure energy. When the deformation of the structure exceeds the elastic limit, the structure will undergo plastic

deformation. After unloading, the deformation of the structure cannot be completely recovered and there will be residual deformation and energy dissipation. According to "The technical specification for concrete structures of tall buildings," the energy dissipation capacity of specimens should be measured by the area enclosed by the load-displacement curve [11–14]. Figure 5 is a schematic diagram for calculating the energy dissipation and equivalent viscous damping coefficients of specimens.

The energy dissipation factor is the ratio of the energy consumed by a hysteresis loop to load and unload for a circle to the total energy of loading and unloading. The energy dissipation factor E' of the specimen [15–18] can be calculated by formula (5).

$$E' = \frac{S_{A'BC} + S_{CDA'}}{S_{\Delta BOE'} + S_{\Delta DOF'}}. \tag{5}$$

In the force response analysis of prefabricated shear wall structure [19–21], the equivalent viscous damping coefficient h_e is often used to carry out the pressure analysis. The equivalent viscous damping coefficient h_e can be calculated by using the formula (6).

$$h_e = \frac{E'}{2\pi}. \tag{6}$$

Figure 6 is the energy dissipation diagram for each specimen of prefabricated shear wall structure:

According to Figure 6, it can see that with the increase of the displacement, the hysteretic curve of the specimen tends to be full and the energy consumption increases gradually. The energy dissipation capacity of the specimens under high axial compression ratio is relatively large, whether it is the connecting steel or the connecting steel plate in the prefabricated shear wall structure [22–24].

Figure 7 is the diagram of equivalent viscous damping coefficient of each specimen in a prefabricated shear wall structure.

As can be seen from Figure 7, with the increase of displacement, the hysteresis loops of all the specimens in the prefabricated shear wall structure are gradually full, and the equivalent damping coefficient is increasing.

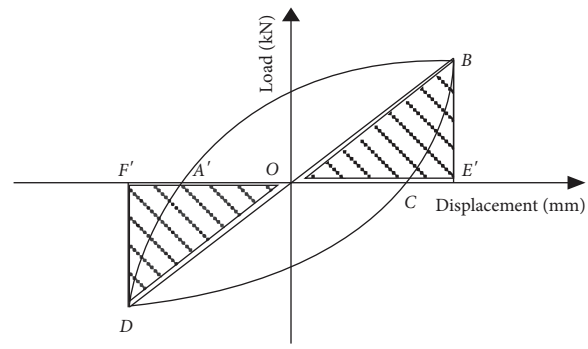

Figure 5: Diagram for calculating energy dissipation and equivalent viscous damping coefficient for prefabricated shear wall structure.

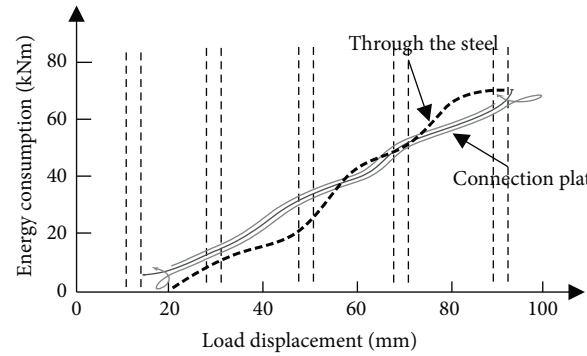

Figure 6: Energy dissipation diagram for each specimen of prefabricated shear wall structure.

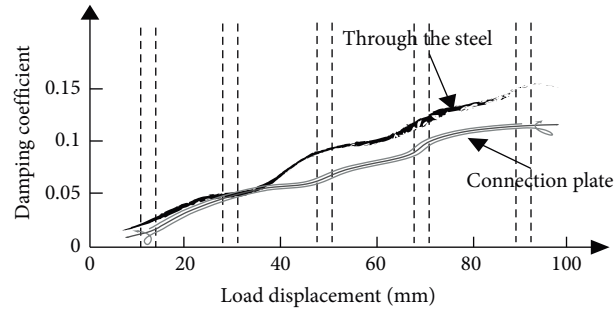

Figure 7: Equivalent viscous damping coefficient diagram of each specimen in prefabricated shear wall structure.

3. Experimental Results and Analysis

In order to verify the correctness of finite element analysis results of prefabricated shear wall structures [25–27], an experiment is needed to verify the above results. The experimental platform is built on MATLAB.

The prefabricated shear wall structure is taken as the experimental object, and the pressure is applied to record and track its bearing changes. The overall experimental results are as follows.

From Figure 8, we can see that the ultimate load of the shear wall finite element simulation is higher than the actual result, because the concrete vibration is not enough, and the specimen maintenance process is not up to standard, but the material in finite element simulation is not defective.

However, the hysteretic curve of the finite element simulation of prefabricated shear wall is quite different from the actual result, and it can be found that the modeling of the finite element is correct.

As shown in Figure 9, the stiffness degradation values in the initial stage of the literature method and the proposed method are in high agreement with the actual values and are in a state of basic level. But with the changing value of displacement, the simulated value of the literature methods gradually deviated from the actual value curve. In the process of small displacement loading, the stiffness of all the specimens in the structure degenerates greatly and the loading continues to continue. The proposed method

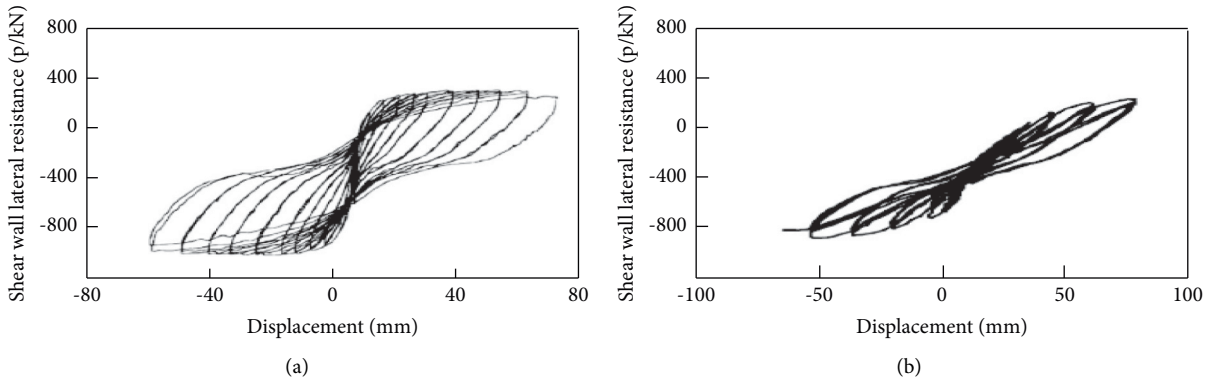

Figure 8: Agreement between hysteretic curve of the shear wall structure by using the proposed method with the actual value. (a) Hysteretic curve of simulated prefabricated shear wall structure and (b) hysteretic curve of actual prefabricated shear wall structure.

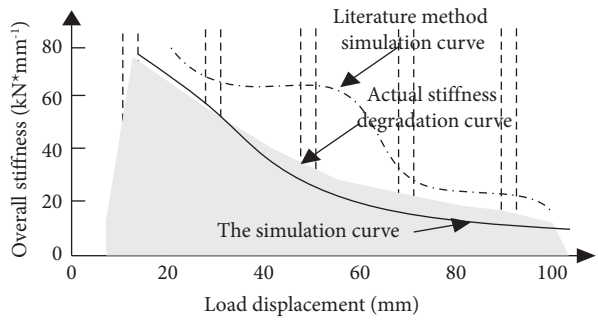

Figure 9: Agreement between simulated values of the overall stiffness degradation of prefabricated shear walls by different methods and actual values.

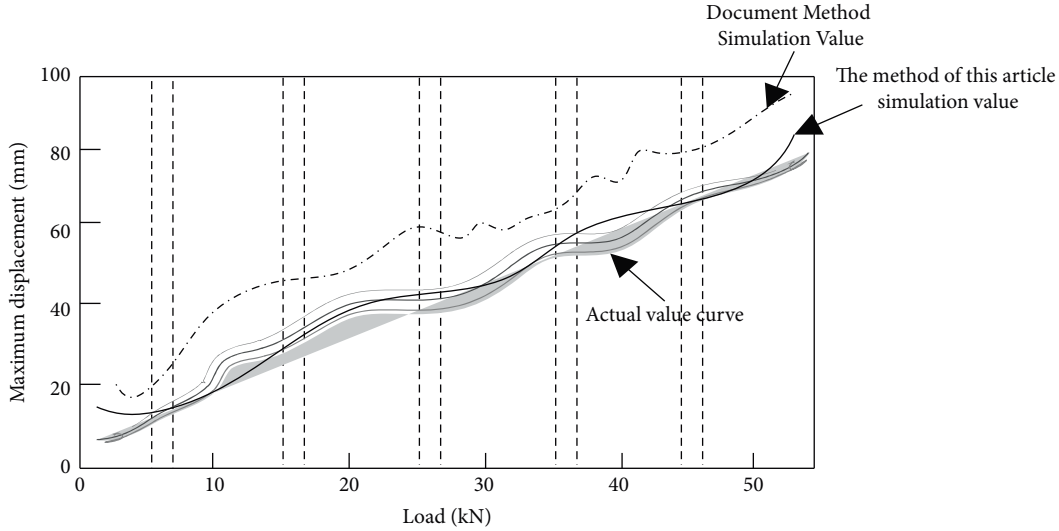

Figure 10: The fitting degree of the maximum displacement and load relation between the simulated value of the different methods and the actual value.

presents the advantages and is in a relatively consistent state with the actual stiffness degradation curve.

Figures 10–13show the fitting degree of the maximum displacement and load relation between simulated values of different methods and actual values; the fitting degree of the maximum strain and displacement relationship between the simulated value of different methods and the actual value; the fitting degree of the simulated values of different methods and the actual values between the stress distribution and the load relation; the fitting degree of the displacement changes of different methods and the actual value under the different friction coefficients.

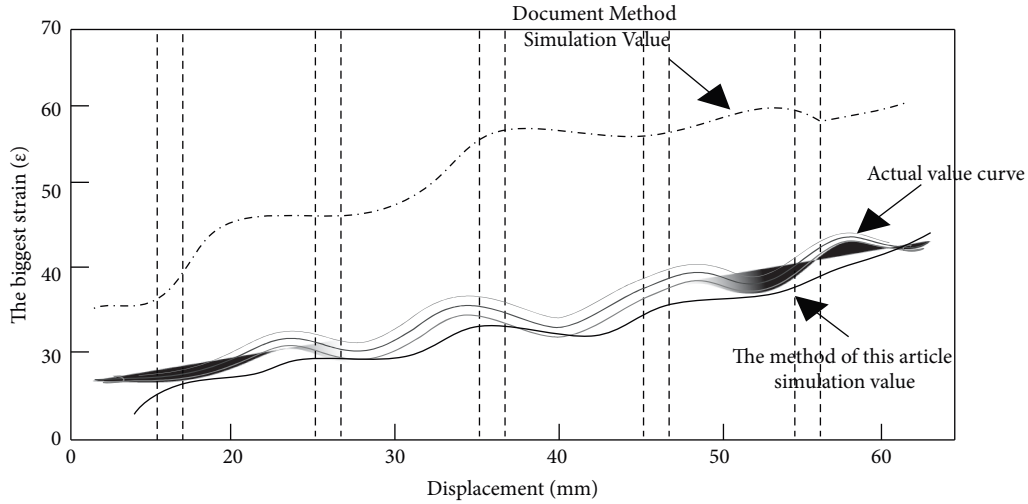

Figure 11: The fitting degree of the maximum strain and displacement relation between the simulated values of different methods and the actual values.

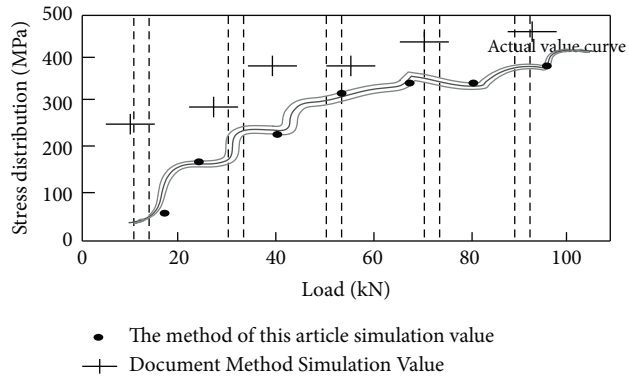

Figure 12: The fitting degree of stress distribution and load relation between the simulated values of different methods and the actual values.

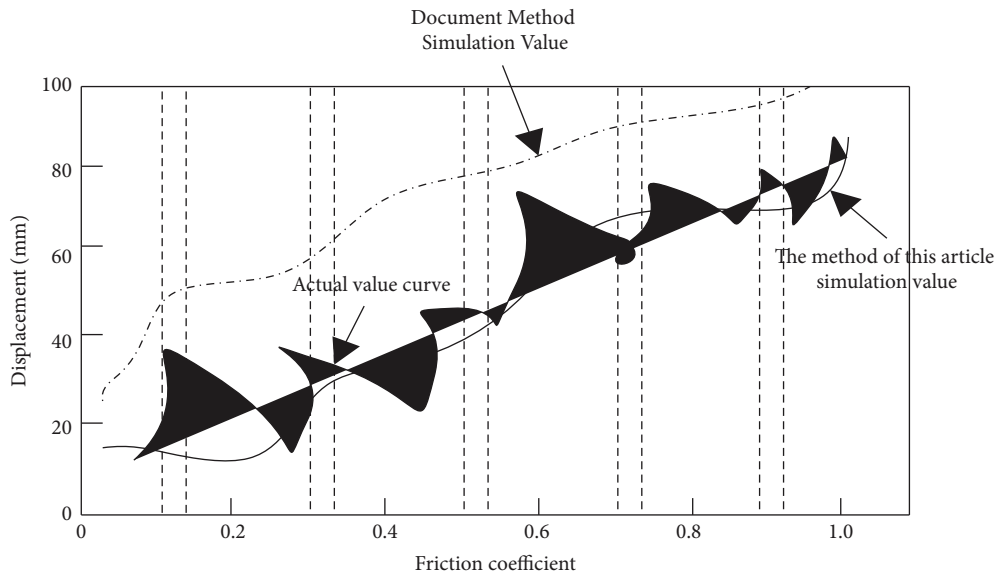

Figure 13: The fitting degree of the displacement changes of different methods and the actual value under the different friction coefficients.

The analysis of Figures 10–13 shows that the simulated value of the maximum displacement and load relation of the proposed method are fitted to the actual value. The maximum strain and displacement relation between the simulated value and the actual value is fitted, and the relationship between stress distribution and load relation of the simulated value and the actual value is fitted. The fitting degree of the displacement changes of different methods and the actual value under the different friction coefficients is better than that of the literature method. This is because in the establishment of finite element model of prefabricated shear wall structure, the grid is divided by using sweep grid division, the control of grid precision is within 100 mm, and the force analysis of the model is always carried out according to "The technical specification for concrete structure of high rise buildings." Moreover, the energy dissipation of shear wall structure and the equivalent viscous damping coefficient are analyzed in detail, and the overall analysis accuracy of the method is improved.

4. Conclusions

Prefabricated shear wall structure is a highly applied energy-saving building material. Its stress performance analysis is the key to promote the development of technology in this field. At present, there are various problems in the analysis of the force performance. Aiming at these problems, this paper puts forward a new research method, to construct the finite element model of prefabricated shear wall structure by using the ANSYS and prove the feasibility of the proposed method through experiments, which can provide a scientific basis for the development of this field.

Data Availability

The dataset can be accessed upon request.

Conflicts of Interest

The author declares that there are no conflicts of interest.

References

[1] W. J. Li and Q. Zheng, "Analysis of dynamic response for concrete wall under blast load," *Computer Simulation*, vol. 33, pp. 27–31, 2016.

[2] M. Heidari, M. A. Nikolinakou, P. B. Flemings, and M. R. Hudec, "A simplified stress analysis of rising salt domes," *Basin Research*, vol. 29, no. 3, pp. 363–376, 2016.

[3] A. F. Liu and J. J. Gurbach, "Application of a p-version finite element code to analysis of cracks," *AIAA Journal*, vol. 32, no. 4, pp. 828–835, 1994.

[4] M. Essuri, B. Maatug, and K. Kurmaji, "Stress analysis of delta fin structure and determination of deformation," *Physics of Plasmas*, vol. 21, pp. 122–143, 2015.

[5] A. L. Zhang, L. Ma, X. C. Liu, and Z. Q. Jiang, "Finite element analysis on mechanical performance of steel frame structure with prefabricated external wall panel," *Journal of Building Structures*, vol. 37, pp. 152–157, 2016.

[6] T. Giesa, C. C. Perry, and M. J. Buehler, "Secondary structure transition and critical stress for a model of spider silk assembly," *Biomacromolecules*, vol. 17, no. 2, pp. 427–436, 2016.

[7] M. Ohsaki, T. Miyamura, M. Kohiyama, T. Yamashita, M. Yamamoto, and N. Nakamura, "Finite-element analysis of laminated rubber bearing of building frame under seismic excitation," *Earthquake Engineering & Structural Dynamics*, vol. 44, no. 11, pp. 1881–1898, 2015.

[8] O. Salomón, S. Oller, and A. Barbat, "Finite element analysis of base isolated buildings subjected to earthquake loads," *International Journal for Numerical Methods in Engineering*, vol. 46, pp. 1741–1761, 2015.

[9] G. Wang, "J integral finite element analysis for three-dimensional cracks," *Journal of Aircraft*, vol. 21, no. 11, pp. 899–905, 1984.

[10] C. García, G. N. Gatica, and S. Meddahi, "Finite element semidiscretization of a pressure-stress formulation for the time-domain fluid-structure interaction problem," *IMA Journal of Numerical Analysis*, vol. 37, pp. 1772–1799, 2017.

[11] H. Xu, J. Song, D. An, Y. Song, and X. Lv, "Local thickening and friction reducing to constant resistance in a prefolded energy absorption device," *Shock and Vibration*, vol. 2020, Article ID 8532534, 11 pages, 2020.

[12] L. H. Li, J. C. Hang, Y. Gao, and C. Y. Mu, "Using an integrated group decision method based on SVM, TFN-RS-AHP, and TOPSIS-CD for cloud service supplier selection," *Mathematical Problems in Engineering*, vol. 2017, Article ID 3143502, 14 pages, 2017.

[13] N. Li, Z. Ma, P. Gong, F. Qi, T. Wang, and S. Cheng, "Simulation research on the load transfer mechanism of anchoring system in soft and hard composite rock strata under tensile loading conditions," *Advances in Materials Science and Engineering*, vol. 2020, Article ID 9097426, 20 pages, 2020.

[14] L. Li, T. Qu, Y. Liu et al., "Sustainability assessment of intelligent manufacturing supported by digital twin," *IEEE Access*, vol. 8, pp. 174988–175008, 2020.

[15] L. Yan, J. Liang, and W. Li, "Axial compression behavior of rubberized concrete-filled square steel tubular columns after exposed to high temperatures," *Advances in Materials Science and Engineering*, vol. 2022, Article ID 1506483, 7 pages, 2022.

[16] L. Li, B. Lei, and C. Mao, "Digital twin in smart manufacturing," *Journal of Industrial Information Integration*, vol. 26, no. 9, Article ID 100289, 2022.

[17] J. X. Li, J. T. Wang, Q. Sun, Y. R. Wu, S. M. Zhou, and F. C. Wang, "Axial compression behavior of circular concrete-filled high-strength thin-walled steel tubular columns with out-of-code D/t ratios," *Advances in Materials Science and Engineering*, vol. 2021, Article ID 9081566, 16 pages, 2021.

[18] Z. Ding, J. Fu, X. Li, and X. Ji, "Mechanical behavior and its influencing factors on engineered cementitious composite linings," *Advances in Materials Science and Engineering*, vol. 201915 pages, Article ID 3979741, 2019.

[19] L. Li and C. Mao, "Big data supported PSS evaluation decision in service-oriented manufacturing," *IEEE Access*, vol. 8, pp. 154663–154670, 2020.

[20] X. Li, C. Ji, Z. Zhang, S. Zhang, H. Liu, and S. Wang, "Shulin.Prediction of adhesively bonded polyurethane-to-steel double butt joint failure using uncertainty analysis," *Advances in Materials Science and Engineering*, vol. 202013 pages, Article ID 3196345, 2020.

[21] L. Li, C. Mao, H. Sun, Y. Yuan, and B. Lei, "Digital twin driven green performance evaluation methodology of intelligent manufacturing: hybrid model based on fuzzy rough-sets AHP,

multistage weight synthesis, and PROMETHEE II," *Complexity*, vol. 2020, no. 6, pp. 1–24, Article ID 3853925, 2020.

[22] S. Zhang, Z. Ren, Z. Ding, J. Wen, and Z. Yan, "Influence of existing defects on mechanical properties of NC lining," *Advances in Materials Science and Engineering*, vol. 2019, Article ID 8571297, 15 pages, 2019.

[23] S. Nie, T. Zhou, Y. Zhang, B. Zhang, and S. Wang, "Shuo.Investigation on the design method of shear strength and lateral stiffness of the cold-formed steel shear wall," *Mathematical Problems in Engineering*, vol. 2020, Article ID 8959712, 13 pages, 2020.

[24] J. Wang and Q. Sun, "Experimental study on improving the compressive strength of UHPC turntable," *Advances in Materials Science and Engineering*, vol. 2020, Article ID 3820756, 21 pages, 2020.

[25] L. H. Li, J. C. Hang, H. X. Sun, and L. Wang, "A conjunctive multiple-criteria decision-making approach for cloud service supplier selection of manufacturing enterprise," *Advances in Mechanical Engineering*, vol. 9, no. 3, Article ID 168781401668626, 2017.

[26] A. Tessler, R. Roy, M. Esposito, C. Surace, and M. Gherlone, "Shape sensing of plate and shell structures undergoing large displacements using the inverse finite element method," *Shock and Vibration*, vol. 2018, Article ID 8076085, 8 pages, 2018.

[27] L. W. Zhang, J. Wu, and D. L. Zhang, "Shape optimization and stability analysis for kiewitt spherical reticulated shell of triangular pyramid system," *Mathematical Problems in Engineering*, vol. 2019, Article ID 2723082, 11 pages, 2019.